

David W. Roberts, Gary G. Gimmestad, John M. Stewart
 Georgia Tech Research Institute, Atlanta, Georgia

1. INTRODUCTION

All ground-based astronomical observational data include effects of the Earth's atmosphere, which is a wavelength dependent, spatially and temporally non-stationary optical medium. The atmosphere creates two different physical types of observational effects: it absorbs and scatters light in a wavelength dependent manner, and it blurs images by turbulence-induced refractive wave front perturbations. Adaptive optics significantly reduces the effect of turbulence, but extinction from scattering and absorption is not currently being measured to high precision. Astronomical sites often incorporate ingenious techniques for estimating atmospheric extinction, such as dedicated photometric telescopes and radiometers, but these techniques are based on stellar measurements that average over long time periods during the night as the light from the celestial object being monitored passes through the atmosphere over a range of angles. Atmospheric variability during the averaging period will reduce measurement accuracy, however. The lack of precision, high-speed atmospheric characterization often leads to less than optimum utilization of expensive telescope resources.

Ground-based stellar photometry measurements are made in the visible and near-infrared wavelength region. Atmospheric extinction at these wavelengths is due to both gases and particulate matter. The gases that make up 99% of the atmosphere, N_2 and O_2 , have well-established extinction spectra and are not highly variable in time. The stratospheric ozone layer causes a significant mid-visible absorption that is somewhat variable, but the main source of variable extinction is caused by airborne particulates: boundary layer aerosols; dust or smoke in the free troposphere; cloud particles, especially ice crystals in sub-visual cirrus clouds; and stratospheric aerosols, which are currently at

a minimum due to a lack of recent volcanic eruptions. Visible-light lidar is well suited for detecting and mapping particulates, and this fact suggests that a properly designed lidar system will be a valuable adjunct to ground-based stellar photometry.

The Georgia Tech Research Institute (GTRI) is developing a lidar system specifically to support ground-based astronomy. The Astronomical Lidar for Extinction (ALE) will support the second generation of the CCD Transit Instrument with Innovative Instrumentation (CTI-II) at the McDonald Observatory in West Texas. CTI-II is a stationary 1.8 meter meridian-pointing telescope being developed by the University of New Mexico (UNM) (McGraw et al. 2006) that will perform millimagnitude photometry and milliarcsecond astrometry. These measurements will enable a large number of astrophysical research programs including galactic astronomy based upon motions and parallaxes of stars in the solar neighborhood, discovery and synoptic monitoring of black-hole related variability in the cores of galaxies, and the discovery of targets of opportunity based upon either luminosity variability (e.g. supernovae) or motion (e.g. asteroids and comets). Precision measurements of atmospheric extinction are required for the photometric measurements, and air density measurements may help increase the precision of the astrometric measurements. ALE will provide the extinction measurements as well as air density measurements from the magnitude of the Rayleigh return.

2. PERFORMANCE CONSIDERATIONS

Even though ALE will provide measurements for a stationary, meridian-pointing telescope, the technology is being developed with other astronomical applications in mind. Ground-based astronomical measurements can benefit from atmospheric extinction measurements at many points over the sky dome, in real time, throughout a range of visible and infrared wavelengths. Satisfying all of these requirements would lead to an instrument that would be expensive, complex, and would require a powerful laser that creates an eye hazard for aircraft. To

* *Corresponding author address:* David W. Roberts, Georgia Tech Research Institute, Electro-Optical Systems Laboratory, 925 Dalney Street, Atlanta, GA 30332; e-mail: david.roberts@gtri.gatech.edu

reduce the cost and complexity of the instrument, a single wavelength is used with the wavelength dependence of extinction inferred from the type of particulate. Particulate type in a layer will be inferred from the layer's altitude, which is the easiest quantity to measure with lidar. Elastic backscatter operation is chosen for simplicity and low cost.

Eye safety is achieved by using the micropulse lidar technique (Spinhirne 1981). In a micropulse lidar, the beam from a high pulse repetition frequency (PRF) laser with a low pulse energy is expanded to a large diameter to keep the intra-beam power density below the eye safe limit. Adequate measurement accuracy is obtained by averaging the signal from a large number of pulses, typically 10^5 or more. Micropulse lidar technology is usually very sophisticated because sky background photons in the signal must be minimized by using both a very narrow receiver field of view (FOV) and a very narrow bandpass optical filter that must be thermally stabilized. Astronomical measurements are only made at night, however, and the low sky background allows the lidar design to be simplified by using a large FOV and a simple, low-cost optical interference filter. The large FOV simplifies the mechanical design and allows critical transmitter-to-receiver alignment stability to be achieved at a reasonable cost.

Measurements will be performed in the zenith direction and at 30 and 60 degrees off-zenith at eight equally-spaced azimuth directions, for a total of 17 directions. Repeating this measurement set three times per hour only allows approximately one minute for signal averaging in each direction. Profiles to an altitude of 30 km include the entire stratospheric aerosol layer and drive the maximum range requirement to 60 km at 60 degrees off the zenith. The need for precise measurements at long ranges with a one-minute measurement time cannot be met by conventional micropulse lidars, which utilize 20 cm diameter optics and transmitted pulse energies of approximately 10 μ J. In order to meet the measurement time and range requirements it is necessary to increase both the transmitted pulse energy and the receiver collecting area.

The SNR for a background-limited lidar measurement is given by

$$SNR = \frac{n_L}{\sqrt{n_L + n_s}} \quad (1)$$

where n_L is the number of photoelectrons produced by backscattered laser photons incident

on the photodetector and n_s is the number of sky background photoelectrons. In the absence of sky background photons, the SNR increases as the square root of the number of backscattered photons collected by the receiver. Eq. (1) is based on photon statistics and represents the maximum SNR value achievable. ALE will initially employ analog signal processing and so its actual SNR values may be somewhat lower due noise in the preamplifiers and digitizers. ALE may be upgraded to photon counting in the future.

The number of photoelectrons produced by laser photons received in a range bin is predicted by the lidar equation modified to include the quantum efficiency η of the photodetector,

$$n_L(R) = N_0 k \eta \left(\frac{A}{R^2} \right) \left(\frac{c\tau}{2} \right) \beta(R) \exp \left[-2 \int_0^R \alpha(r) dr \right] \quad (2)$$

where

- $n_L(R)$ = # of photoelectrons generated by photons from range R
- N_0 = number of photons transmitted
- k = receiver optical efficiency
- η = photodetector quantum efficiency
- A = receiver area
- R = range to the scattering volume
- c = speed of light
- τ = range bin duration
- β = atmospheric backscatter coefficient
- α = atmospheric extinction coefficient.

The number of sky background photoelectrons per range bin is calculated from

$$n_s = k \eta L_{sky} \Omega_{FOV} A \tau \quad (3)$$

where

- n_s = number of photoelectrons produced by collected sky photons
- L_{sky} = sky radiance in photons/sec m^2 sr
- Ω_{FOV} = receiver field of view solid angle.

Equations (1), (2), and (3) were used in ALE performance simulations.

3. LIDAR SYSTEM DESIGN

ALE will be operated in support of astronomical measurements and cannot have personnel dedicated to it, so it must be capable of fully automated operation. Lidar measurements require all of the laser pulse energy to be contained within the receiver field of view in order

for accurate analysis, so transmitter-to-receiver alignment stability is critical, especially for a system like ALE that must be able to point anywhere in the sky dome above a 60 degree zenith angle.

3.1 TRANSMITTER DESIGN

The transmitter must generate pulses of sufficient energy to permit measurements to the maximum required range with one-minute averaging while keeping the intra-beam pulse energy density below the maximum permissible exposure limit for eye safety. It must reduce the raw beam divergence of the laser enough so that the laser pulse fits within the field of view of the receivers above the lowest altitude of interest. It must also have a high transmission to minimize the size and cost of the laser.

Because ALE will operate at zenith angles up to 60°, the laser PRF is an important factor because the path length to a layer at a 30 km altitude doubles when moving from the zenith to a 60° zenith angle. If the laser PRF is high enough, it is possible for two laser pulses to be in the atmosphere simultaneously during data acquisition. Limiting the PRF to no more than 1500 Hz yields a range redundancy limit of 90 km and ensures that only one pulse at a time will be in the atmosphere below 30 km during a measurement. The Photonics Industries DC10-527 nm Nd:YLF laser selected for ALE produces 100 µJ per pulse at 1500 Hz.

The maximum eye safe fluence at 527 nm is approximately 0.1 µJ/cm² at a PRF of 1500 Hz, but the raw laser beam has a diameter of only 0.6 mm. The extremely small beam must be expanded drastically in order to stay below the eye-safe energy density level. Cassegrain-type telescopes are frequently used for large-aperture beam expanders, but the central obstruction of these telescopes blocks 30% or more of the transmitted pulse energy because the majority of the pulse energy is concentrated in the center of the beam. The high cost of laser photons and the long measurement paths needed require the transmitter optics to have high efficiency, so an unobstructed transmitter design was developed.

Off-axis beam expander designs are frequently based on paraboloidal mirrors, which are expensive and alignment sensitive. In order to minimize costs and reduce alignment sensitivity, only spherical surfaces were used in the beam expander. The expander is divided into two expansion sections: a pre-expander and a main expander. The main expander is based on a Galilean design with a negative diverging lens and

a spherical collimating mirror shown in Figure 1. Shifting the laser beam off-axis so that there is no central obstruction as shown in Figure 2 allows the exiting beam to pass beside the diverging lens. A small amount of the pulse energy is blocked in the region of the diverging lens, but this loss is less than 1% because the energy density at the edge of the primary mirror is lower than at the center. Residual aberrations are small compared to the lidar receiver's field of view, and because an off-axis sphere is the same as an on-axis sphere, the extra cost of fabricating an off-axis mirror is avoided.

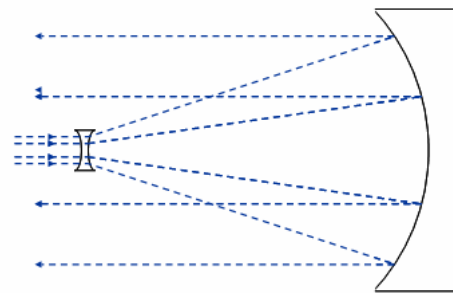


Figure 1. Obstructed Galilean beam expander.

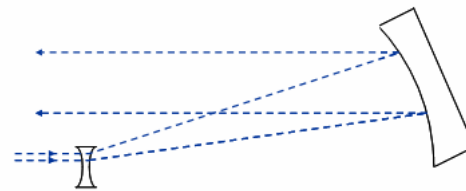


Figure 2. ALE's off-axis beam expander

Spherical aberration is the primary aberration to be corrected in the main expander, and its diverging lens must have a specific power and ratio of surface curvatures in order to offset the spherical aberration of the primary mirror. When the aberrations are minimized, the resulting beam expansion magnification is insufficient to properly fill the collimating mirror aperture and an additional magnification stage is required. This is the function of the pre-expander, a simple Keplerian design that provides the additional magnification to match the laser beam to the off-axis main expander, as shown in Figure 3.

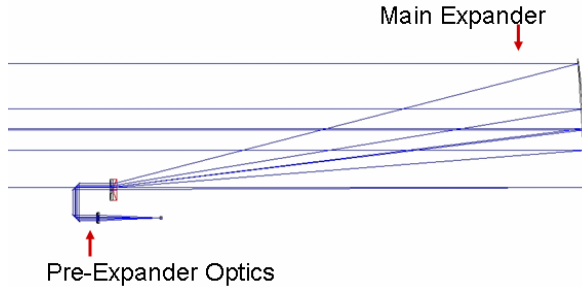


Figure 3. The optical layout of ALE's off-axis transmitter

The resulting optical system is compact and results in a rugged package that will maintain optical alignment. The 3.5 mrad raw laser beam divergence is reduced to 90 μ rad and the transmitted pulse energy is limited only by reflection losses from lens and mirror surfaces, as well as a slight loss of power due to the beam overfilling the primary mirror. ALE's transmitter parameters are summarized in Table 1. The transmitter and short range receiver assembly are shown in Figure 4.

Table 1. Transmitter Parameters

Parameter	Value
Laser type	Nd:YLF
Wavelength	527 nm
Transmitted energy	79 μ J
PRF	1500 Hz
Pulse width	24 ns
Beam divergence	90 μ rad
Output beam diameter	32 cm

3.2 RECEIVER DESIGN

One of the many challenges in designing a lidar is to accommodate the extreme dynamic range of the backscattered signal. As can be seen in Eq. (2), the number of collected photons will drop by a factor of nearly 10^6 between ranges of 100 meters and 90 km due to the $1/R^2$ range factor alone. Because the magnitude of the Rayleigh signal is directly proportional to air density, the dynamic range is increased by an additional factor of $\sim 10^2$ by the decrease in air density with altitude between the observatory at 2076 m MSL and an altitude of 30 km.

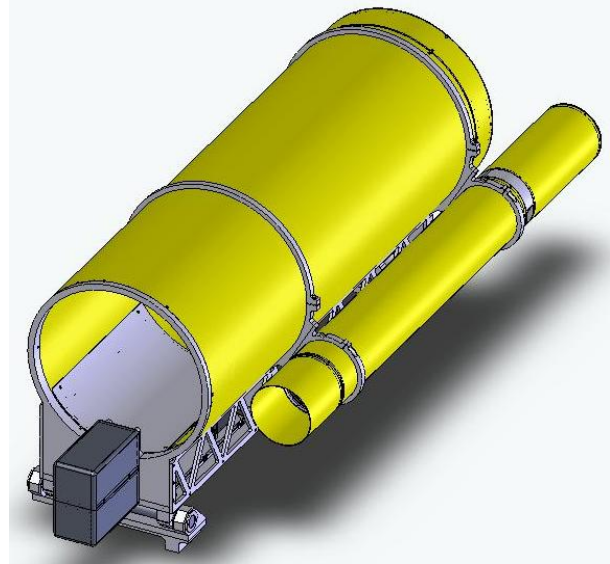


Figure 4. The short-range receiver mounted on the transmitter assembly

Finally, atmospheric extinction on a clear night can increase the dynamic range by another factor of approximately two. ALE uses two receiver telescopes to span the dynamic range: a short-range receiver to handle the higher-intensity signals from low altitudes and a long-range receiver optimized for the lower-intensity returns from high altitudes. The optical design of the detector module is the same for both receivers, as are the photomultipliers (PMTs). Parameters for the short and long-range receivers are summarized in Table 2.

As shown in Figure 4, the short-range receiver is a refractive telescope that is mounted on the side of the transmitter beam expander. Coarse alignment for the short-range receiver is performed by shimming in order to make the alignment as stable as possible by eliminating adjustments on large assemblies that can drift over time. Fine alignment of the short range receiver with the transmitter is performed by moving the field stop laterally relative to the optic axis of the objective lens.

Table 2. Receiver Parameters

Parameter	Short Range	Long Range
Aperture	9.5 cm	67 cm
Focal length	80 cm	724 cm
f/#	8.4	10.8
Field of view	4 mrad	1.5 mrad
Optical efficiency	92%	76%
Range coverage	0.1 – 5 km	5 - 90 km

The transmitter and short range receiver assembly will be mounted on the top of a 67-cm aperture f/10.5 Ritchey-Cretien astronomical telescope carried by an elevation-over-azimuth mount. In addition to serving as the steerable mount for ALE, it also serves as the long range receiver collection optics. This observatory-grade telescope, shown in Figure 5, was originally constructed by an advanced amateur astronomer in the early 80's before it was donated to UNM (Flint 1984). It is currently being refurbished by UNM and will initially be installed at the UNM campus observatory in Albuquerque, New Mexico during ALE's testing phase. Telescopes in this aperture range are often available at observatories and are frequently underutilized, which makes the ALE concept very easy to implement in existing facilities without requiring the purchase of a large aperture instrument for the long range receiver.



Figure 5. The UNM telescope shortly after construction in the early 80's

The detector modules for the long and short range receivers are identical in design. Backscattered photons collected by the receiver

telescope pass through a field stop, a filter, and two lenses before they enter the PMT, as shown in Figure 6. The rays are color coded by field angle, with the green rays corresponding to the edge of the field of view and the blue rays to the center of the field of view. The field stop limits the field of view in order to reduce the number of sky background photons collected by the receiver and also to prevent PMT saturation by defining the lowest altitude where light from the laser pulse enters the field of view. The 1.5 mrad long-range receiver FOV and the 4 mrad short-range FOV are large by conventional micropulse lidar standards, but they are crucial to the alignment stability of ALE because they make the system much less sensitive to small changes in the mechanical alignment between the transmitting telescope, the short range receiver telescope, and the long range receiver telescope.

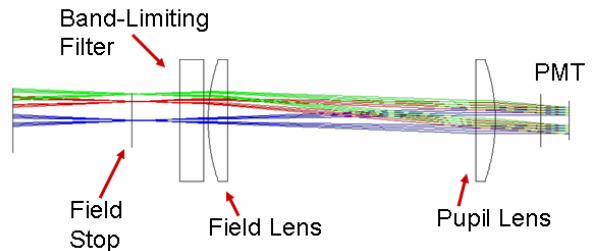


Figure 6. The optical layout for the short and long-range receiver detector modules

The receivers use Licel-packaged Hamamatsu compact metal package photomultipliers (PMTs) and Licel low-ripple high voltage power supplies. Each receiver incorporates a high efficiency, 30 nm wide bandpass filter to further exclude moonlight, night sky emission, and light pollution, and to minimize the effect of stars that cross the field of view during a measurement. The filter bandpass is significantly wider than that for traditional lidars, but because ALE will only be operated at night, the wider bandpass is adequate and the filter provides twice the peak transmission of a filter with a bandpass appropriate for daytime use. The field lens controls the divergence of the light cone passing through the field stop and prevents the light cone from overfilling a lens that images the aperture stop onto the PMT photocathode. Placing a pupil on the photocathode prevents spatial non-uniformities in photocathode sensitivity from introducing range-dependent artifacts into the data. The extreme simplicity of the receiver optical design provides high transmission by

minimizing the number of optical surfaces. The short-range receiver has an optical efficiency of 92%, and the long-range receiver has a total transmission of 76%. The lower long-range receiver efficiency is caused by the aluminized primary and secondary mirror reflectivities and the secondary mirror obstruction of the Ritchey-Chretien telescope.

3.3 DATA SYSTEM

The PMT output currents are converted to a voltage by custom transimpedance preamplifiers and the resulting signal is digitized by an analog-to-digital converter (ADC). Data system design is challenging due to the combination of high maximum range, large signal dynamic range, and high laser PRF. The high PRF is particularly challenging because transferring data from the ADC memory to the data system PC memory takes a significant amount of time. The data transfer problem was eliminated by selecting the Gage Applied Technologies Model 14200 ADC, which performs multiple-pulse averaging on the digitizer card and transfers only the averaged data to the PC. The 14200 is a two-channel, 14-bit, high-speed analog to digital converter that has the capability to average up to 1024 laser pulses. For ALE, both receiver signals are digitized at 10 million samples per second to provide 15-meter range bins. A total of 6,000 range bins are used to provide a 90 km maximum range. LabVIEW-based software controls the ADC and processes the averaged atmospheric profiles. Low-level data processing functions performed by LabVIEW include background subtraction, filtering and down-sampling the averaged data, adding the processed result to a long term sum, and averaging many samples to further improve the SNR. The data system provides accurate data over the full dynamic range of the backscattered lidar signal ranging from the low photon arrival rates at long ranges (~ 100 photons/sec) while accommodating the high arrival rates from short ranges ($\sim 10^9$ photons/sec).

4. ALE OPERATION

For elastic backscatter lidar, the most robust technique for obtaining extinction values in absolute units is to employ zenith angle scans in a technique similar to the Langley plot used in sun photometry. If one compares the signal from a given altitude layer at two different zenith angles, it is possible to determine the transmittance of all layers below that altitude. In practice,

measurements at a few zenith angles from 0° to 60° are required to produce an accurate estimate of the transmission. The only assumptions behind this technique are that the atmosphere is horizontally homogeneous and that it does not change during the scan. The data provides a limited self-consistency check on these assumptions in that the data points should lie on a straight line in the lidar Langley plot. The technique has been extensively studied during daytime to measure aerosol extinction in the well-developed mixing layer, which is characterized by large eddies with a horizontal extent of approximately 1.5 times the mixing layer depth. The existence of these eddies practically guarantees that the requirement for horizontal homogeneity will not be met, and much field experience has shown this to be the case. Russell and Shaw (1975) have also pointed out that data with time or angle-dependent artifacts can still yield straight lines on Langley plots, so the existence of good linear fits is necessary but not sufficient for establishing accuracy.

By contrast, the nighttime boundary layer aerosols are typically stratified, so the "lidar Langley plot technique" might be expected to give much better results at night. Unfortunately, nighttime lidar Langley plots are uncommon in the literature. Nighttime Langley plots have been used extensively by astronomers at the Big Bear Solar Observatory in California using the moon as the light source, and their results show inconsistencies as large as $\pm 20\%$ from month to month (Qiu et al. 2003). They attributed these discrepancies to hemispherical shells of aerosols over their site, but a much more likely explanation is that the aerosol extinction changed during the data acquisition, which was typically four to six hours long. If this explanation is correct, the Big Bear results illustrate the need to use a lidar rather than celestial sources in order to complete the scans on an appropriate time scale. In any event, the nighttime behavior of the aerosol layer will be site specific, and traditional nighttime-only astronomical sites are quite different from the Big Bear solar site.

Another common approach to analyzing lidar data is to assume that the ratio of the extinction and backscatter coefficients, α/β , has a constant value. Then the lidar equation can be inverted, assuming a value for the extinction coefficient at the far end of the range (Klett 1981). Generally, the assumptions behind this approach have unknown validity, and there is no self-consistency check. However, inversions can be used in combination with the zenith angle scans in

an iterative scheme to determine α/β within approximately $\pm 10\%$. Then the lidar can remain pointing at the zenith and the data can be inverted with more confidence. This combination of techniques will be ideal for a boundary layer at a Southwestern observatory site, where the properties of the desert aerosol are fairly constant. A year of observations will reveal seasonal and annual variations.

Cirrus is a different problem, because the optical properties of cirrus are variable and the clouds are characterized by their wispy, inhomogeneous structure. A standard method of estimating cirrus transmittance is to measure the Rayleigh backscatter signal from molecules above and below the cloud, and to attribute any decrease to the transmittance of the cloud. This technique requires that the measurement interval and pointing direction of the lidar match those of the astronomical instrument very closely. An important contribution of ALE may be simply to alert observers to the presence of such clouds in the optical path.

The lidar control system will be remotely accessible by a secure Internet connection when ALE is permanently installed at McDonald Observatory. ALE can be directed to carry out specific operations (e.g. scan or shut down), make specified measurements or enter an operating mode by means of a local or remote-operator command. In autonomous operation, ALE's typical operating mode, CTI-II will direct the lidar's operation. Time synchronization will be provided to ALE by the observatory using the Internet connection.

ALE will have a number of operating modes. A go/no-go observing decision mode will require ALE to quantitatively measure zenith extinction. ALE will detect one or more layers of extinction corresponding to clouds, aerosols, smoke, dust or other extinction sources during this initial observation. If the total extinction is sufficiently low that astronomical observations are possible, ALE will automatically begin sky dome mapping measurements.

To map the sky dome, ALE acquires a series of profiles in eight azimuth directions to detect particulates and quantitatively estimate the extinction as a function of air mass. These observations will normally be made at the beginning of the night prior to making decisions about whether to open telescopes for observing, and will affect the type of observation: photometric, astrometric, high value variability estimates, etc.

The altitude of particulate layers will allow the particulate type to be inferred so that a layer's extinction wavelength dependence can be estimated. The various calibrations and extinction records will be maintained as part of the engineering data stream of the observatory.

5. TEST PLANS

The ALE system will undergo several stages of testing. The first stage will occur as ALE is assembled at GTRI in Atlanta. At that point, ALE will not be mounted on a telescope and will lack a long-range receiver and scanning capability, but the tests will allow the system to be checked out thoroughly.

The second stage of testing will be performed at the Bradley Observatory at Agnes Scott College (ASC), a women's college in Atlanta. The Bradley 30-inch Classical Cassegrain telescope will serve as a surrogate for the Ritchey-Chretien telescope while ALE is put through its paces. The ASC tests will verify the performance of both short and long-range receivers and it will provide nighttime zenith angle scans.

Because the magnitude of horizontal inhomogeneity in the nighttime boundary layer aerosol is generally unknown, measurements are being performed at ASC with the vertically-pointing micropulse Eyesafe Atmospheric Research Lidar (EARL). EARL was developed by GTRI for undergraduate research and education at ASC (West et al. 2006). Prevailing winds transport the aerosol layer through the vertical beam and enable aerosol variability to be observed by doing continuous measurements over a period of time. EARL will be operated during ALE's second testing phase to gather supporting data.

The third phase of testing will take place at the UNM campus observatory and will be a full-up test of the complete ALE system including its shelter and software. After testing is completed, ALE will be ready for installation and routine operation at McDonald Observatory in support of CTI-II.

6. CONCLUSIONS

A rugged, eye safe lidar system known as the Astronomical Lidar for Extinction has been developed specifically to support observations made with the second generation CCD Transit Instrument with Innovative Instrumentation, a unique 1.8 meter survey telescope currently under design that will be operated at McDonald

Observatory. ALE will be operated to support the precision astrometric and photometric observational programs enabled by this telescope, and it is currently undergoing a series of tests. A performance analysis indicates that it will provide very useful quantitative characterization of the Earth's atmosphere that has never before been available to astronomers, demonstrating that lidar technology is invaluable at any observatory. Many observatories have an unused telescope in the 16-30 inch range, on a mount in a dome, and often with software for motion control. ALE's transmitter and short-range receiver are modular units that can be adapted to any such telescope with minimal costs. An observatory can put an unused instrument into use to gain greater photometric precision and improve observation scheduling.

Spinhirne, J.D., 1993: Micro Pulse Lidar, *IEEE Transactions on Geoscience and Remote Sensing*, **31**, 48-55.

West, L.L., Gimmestad, G., Bowling, A., Roberts, D., Stewart, J., and Wood, J., 2006: Atmospheric Laser Radar as an Undergraduate Educational Experience, *American Journal of Physics*, **74**, 665-669.

7. ACKNOWLEDGEMENTS

GTRI is developing ALE for UNM with funding from the National Science Foundation under grant number 0421087. We gratefully acknowledge the support of NSF.

8. REFERENCES

Flint, G., 1984: Nearing First Light at the J.R. Frost Observatory, *Sky & Telescope*, 402-405.

Klett, J.D., 1981: Stable Analytical Inversion for Processing Lidar Signals, *Applied Optics*, **20**, 211-220.

McGraw, J.T., M.R. Ackerman, W.H. Gerstle, W.T. Williams, P.C. Zimmer, 2006: The second-generation CCD/transit instrument (CTI-II) precision astrometric and photometric survey, *Proc. SPIE*, **6267**.

Qiu, J., P. R. Goode, E. Pallé, V. Yurchyshyn, J. Hickey, P. Montañés Rodríguez, M.-C. Chu, E. Kolbe, C. T. Brown, and S. E. Koonin, 2003: Earthshine and the Earth's albedo: 1. Earthshine observations and measurements of the lunar phase function for accurate measurements of the Earth's Bond albedo, *Journal of Geophysical Research*, 108(D22), 4709, doi:10.1029/2003JD003610.

Russell, P.B., and Shaw, G.E., 1975: Comments on "The Precision and Accuracy of Volz Sunphotometry", *Journal of Applied Meteorology*, **14**, 1206-1209.